NASA Technical Memorandum 86952

Advanced Liner-Cooling Techniques for Gas Turbine Combustors

Carl T. Norgren and Steven M. Riddlebaugh
Lewis Research Center
Cleveland, Ohio

Prepared for the
Twenty-first Joint Propulsion Conference
cosponsored by the AIAA, SAE and ASME
Monterey, California, July 8-10, 1985

NASA

ADVANCED LINER-COOLING TECHNIQUES FOR GAS TURBINE COMBUSTORS

Carl T. Norgren and Stephen M. Riddlebaugh
National Aeronautics and Space Administration
Lewis Research Center
Cleveland, OH 44135

E-2475

Abstract

Component research for advanced small gas turbine engines is currently underway at the NASA Lewis Research Center. As part of this program, a basic reverse-flow combustor geometry was being maintained while different advanced liner wall cooling techniques were investigated. Performance and liner cooling effectiveness of the experimental combustor configuration featuring counter-flow film-cooled panels is presented and compared with two previously reported combustors featuring: (1) splash film-cooled liner walls; and (2) transpiration cooled liner walls (Lamilloy).

Introduction

Problems unique to small combustors were recently reviewed during a forum at NASA Lewis Research Center conducted by A.D. Little, Inc.[1] The objective of the forum was to identify the R&D effort which must be considered in the 1980 to 1990 time frame to meet the critical needs for small aircraft gas turbines. Improvements in cycle efficiency and reduction in specific fuel consumption were primary considerations. It is possible to achieve improvements in these areas with higher inlet turbine temperature and increased pressure ratio; however, less and hotter air remains for liner cooling. This loss in heat sink capability is particularly critical in the small combustor system due to the inherent high surface-to-volume ratio. It was the consensus of the participants in the forum that liner cooling was one of the most important problem areas that should be considered. Advanced cooling techniques must be incorporated in the combustor in order to achieve the potential for implementing advanced cycles.

As part of a component research program for advanced small gas turbine engines currently underway at the NASA Lewis Research Center, a basic reverse-flow combustor has been used to investigate advanced liner wall cooling techniques. Performance and liner cooling effectiveness of the experimental combustor configuration primarily featuring counterflow film-cooled panels were determined and compared with two previously reported combustors featuring: (1) splash film-cooled liner walls; and (2) transpiration cooled liner walls.

In this study, the design and fabrication of a combustor liner using advanced cooling techniques was patterned after an existing NASA reverse-flow film-cooled design.[2] To maintain internal flow dynamics, the physical geometry, air-entry distribution, and combustor pressure-drop across the liner were similar. The conventional existing splash film-cooled wall was designed using a one-dimensional computational scheme assuming a steady state heat flux balance between the heat gained by the wall and the heat lost.[3] Conduction within the wall and radiation interchange between the hot walls were considered negligible.

The advanced liner cooling configuration was designed and built in joint NASA/Army effort with the Garrett Turbine Engine Company.[4] The advanced liner cooling configuration was based on similar aerothermodynamics of the film-cooled design. The predicted performance of the advanced liner cooling configuration was based on a three-dimensional combustor internal flow analysis to: (1) provide thermal-boundary conditions for analyzing stresses in the combustor walls and the transition liners; and (2) predict the trajectory of the fuel spray to define a liner configuration which would minimize near-wall burning and thus reduce thermally-induced liner stresses. The combustor liner-wall temperature analysis was performed using a one-dimensional computational scheme.

The experimental results are compared with the reference film-cooled combustor and a transpiration cooled (Lamilloy) combustor.[5] Documentation of performance, emission index levels, and liner cooling effectiveness over a range of simulated flight conditions of a 16:1 compression pressure ratio gas turbine engine was obtained.

Apparatus

Test Facility

The test combustor was mounted in a closed-duct facility (Fig. 1). Tests were conducted with inlet-air pressure ranging up to 16 atmospheres with the air indirectly heated to about a temperature of 720 K. The temperature of the air flowing out of the heat exchanger was automatically controlled by mixing the heated air with varying amounts of cold by-passed air. Airflow through the heat exchanger and by-pass flow system and the total pressure of the combustor inlet airflow were regulated by remotely controlled valves as indicated.

Combustors

The reverse flow combustor used in this investigation was patterned after a full-scale experimental design. The design stresses versatility so that the interchanging of fuel injectors and the modification or replacement of the swirlers, faceplate, and liner can be readily accomplished. The airflow distribution and hole sizing of the liner are based on 36 primary and dilution holes. In this investigation three combustors with similar internal aerothermal design, but with different liner wall cooling schemes are compared. The cooling configurations are: (1) splash-film (SF); (2) a pseudo-transpiration liner "LAMILLOY"* (TRANS); and (3) a configuration primarily featuring a counter-flow film-cooled technique (CFFC). Design details and performance of the referenced SF and TRANS designs have been presented in Ref. 5. A

*Trademark.

summary of the design of the CFFC liner relevant to the present investigation follows.

Counter-flow film-cooled (CFFC) liner. The CFFC combustor liner was designed under government contract by the Garrett Turbine Engine Company. The following paragraphs summarize the design procedure for the NASA configuration as presented in Ref. 4.

The baseline configuration was run with airflow distribution as predicted by the Garrett annulus flow program with the predicted jet velocities. A 20° sector of the combustor 11.8 cm long was analyzed by the three-dimensional model. The sector was divided into 32 by 18 by 13 grid points, the center of the fuel nozzle spray being at 10°. The baseline case was run using a simplex-pressure atomizing nozzle with a 25 atmosphere pressure differential, a Sauter Mean Diameter of 30 μm and a fuel spray cone angle of 90°.

Figure 2(a) presents the calculated axial velocity isopleths for an "x-y" plane in-line with the nozzle spray centerline for the original NASA reference combustor. There were two distinct recirculation zones predicted as denoted by the zero velocity lines. Temperature distribution profiles for an "x-y" plane in-line with the fuel nozzle are shown in Fig. 2(b). After the analysis of the reference combustor characteristics, the liner cooling design effort was concentrated on determining the cooling requirements to insure a peak liner temperature less than 1200 K (1700 °F).

Analysis and optimization of the cooling air distribution. The goal for the liner cooling requirements was to reduce the liner-wall temperature by a significant magnitude without modifying the combustion process. The overall geometric envelope of the combustor was preserved, as were the locations and airflow rates of the primary and dilution-zone orifices, and of the dome swirlers. The wall temperatures predicted from a one-dimensional computational scheme indicated severe liner conditions; consequently, three techniques were employed to reduce the wall temperatures to an acceptable level: (1) convective counter-flow film-cooling; (2) rectangular offset-fin plate cooling; and (3) extended surface-film cooling. For each technique, the coolant flowed through convective or fin passages before it was injected into the hot combustion gases. The second cooling scheme was considered only for the cylindrical section of the combustor. The transition liner geometry prohibited the use of offset-fin plates. Considerations for the coolant technique selection for each section of the combustor are presented in the subsequent paragraphs.

Since the coolant film flows through the annulus channel before being injected in the hot combustion gases, an increase in heat transfer was expected if the velocity of the coolant was significantly increased. On the outer liner computations indicated that significant improvements in cooling were achieved; however, the temperature levels remained unacceptably high. On the inner liner, the wall temperature profiles were greatly improved due to the increased flow velocity along the liner wall cold side. The primary and the first-dilution panel required more coolant flow to limit the temperature rise. The second dilution panel displayed a satisfactory temperature profile, but also resulted in a relatively large pressure drop. In order to increase the heat transfer and reduce the pressure drop of the coolant, fins with higher heat-transfer coefficients and larger channel areas were investigated.

The requirements for a small size, lightweight, high performance heat exchanger were adapted from finned wall rocket nozzle technology. The offset fins are geometrically characterized by their density, shape, height, wall thickness, and fin length. An iterative process was established to match airflow distribution with fin performances, temperature reduction, and pressure drop penalties.

The prime objective was to determine among the existing and available offset-fin tooling, a configuration that would ensure acceptable wall temperatures and minimum friction losses. Also taken into account were severe tool manufacturing restrictions in the choice of the shape, ratios of wall thickness to fin height, and maximum fin density (due to the difficulty of forming Hastelloy X fin material).

Different geometrical configurations were investigated to minimize the wall temperature for the least flow penalty. Among these, the original cooling configuration for the outer liner was modified to incorporate the dilution and primary jets by delaying the origin of the cooling channel in the vicinity of the holes. The final fin and channel height configuration was based on producing the most significant wall temperature reductions for a given pressure loss and existing tooling dies.

The cross section of the CFFC liner is shown schematically in Fig. 3. On the outer liner, the primary and first-dilution panels (panels C and B in Fig. 3) were cooled in a counter-flow manner. The second dilution panel (A, as shown in Fig. 3) benefitted from the high velocity in the annulus to reduce the temperature to an acceptable level. Consequently, only a roughening treatment was used on the second-dilution panel to enhance the heat transfer rate which permitted a coolant flow of 1 percent of the combustor airflow.

Along the primary zone of the outer liner, a coolant flow of 7 percent was required to ensure significant temperature reductions. It should be noted that a different fin type (unfortunately not available in hard material) would have allowed a significant reduction in the amount of air spent for cooling (i.e., 5 instead of 7 percent). High-density fins may provide further coolant decrease, if they are developed in the future. The Stanton number (i.e., ratio of the Nusselt number/Reynolds number times Prandtl number) is 30 percent higher for the denser fins. This demonstrates their high potential.

On the inner liner, a parallel-flow film-cooling configuration took advantage of the free-stream dynamic head and prevented excessive pressure loss. The air to be used for subsequent combustion and dilution was also ducted into their respective cooling panels prior to injection to provide additional heat sink capacity. Use of the combustion and dilution air for cooling prior to injection resulted in a more effective liner wall configuration, as shown in panels D and E of Fig. 3.

The selection of the fins as an optimal cooling scheme required a slight change in the amount of air flowing through the swirler, 25.43 instead of 26.93 percent.

Transition liner. The flow distribution in the transition liners was restricted in order to minimize the amount of coolant and used a counter-flow scheme. The considerable difficulty required for the fabrication of transition liners with offset-fin plates prohibited their use in favor of the extended surface cooling technique. The heat-transfer rate over a surface can be significantly increased, by as much as a factor of two, if a rough rather than a smooth wall is presented to the flow. The determination of the roughness height required depends on such parameters as coolant passage geometry and flow Reynolds number. The prediction of the heat-transfer gain through increased turbulence and of the skin-friction penalty through increased drag was examined by relating the Stanton heat-transfer number variation with roughness height. The roughness was related to sand-grain equivalence obtained from a correlation by Dirling.[6] The size of the roughness height was determined to provide high heat-transfer coefficient and low-pressure drop. Several configurations of roughness and spacing were examined. Because the Dirling correlation has been extensively applied to hemispheric and conical roughness, a hemisphere like shape was used. The results of this study were applied to the transition liner application. Because of manufacturing constraints, several equivalent roughness heights (relative to the sand-grain equivalence relationship) were made available for trial fabrication.

A comprehensive investigation was undertaken in the design of the transition liner geometry to ensure an acceptable wall temperature distribution to minimize difficulties in manufacturing and assembly accuracy. The configuration selected, shown in Fig. 3, was arrived at by a combination of cooling, frictional losses, and thermal and stress analysis.

Transition liner thermal and stress analysis. A thermal and stress analysis was undertaken in order to determine the thermal deflections of the outer transition liner flow channel sand slot gaps. Maintaining the specified channel and slot heights was critical to the correct cooling of the outer transition liner. The thermal deflection analysis was performed by applying the transition liner temperature distribution to the finite element model. No temperature variation in the sheet thickness direction was assumed in this analysis. Outer sheet temperatures were calculated based on the cooling flow heat transfer coefficients and temperatures. Radiation was not included between the inner and outer sheets of the transition liner. The thermal deflection indicated problem areas with the original concept for the outer transition liner. For example, at operating temperature growth patterns were such that passage areas could be blocked off and upset the predicted coolant flows. In order to reduce the stresses and deflections, the initial design was modified and new temperature distributions computed. Gaps and dimple locations were specified so that the correct design values would be expected at the operating conditions.

The analysis of the inner transition liner indicated that the original concept would be an acceptable design. A peak temperature of 1100 K (1525 °F) is predicted near the interface of the cylindrical section of the liner with the transition zone.

Counter-flow film-cooled (CFFC) combustor. A photograph of the completed CFFC combustor is shown in Fig. 4. It should be noted that both the outer and inner "cold side" surfaces are composed of a series of overlapping plates. This construction was used to prevent a collapse of the finned walls during expansion and contraction due to temperature gradients. A comprehensive design study was carried out to significantly reduce coolant airflow requirements in a reverse-flow annular combustor. The combination of high performance offset fin plates and extended surfaces have allowed increases in the local convective Stanton number up to a factor of 3.5. The offset fin plates were distributed along the inner and outer cylindrical liners, while the transition liner complex geometry required roughened walls to increase the heat transfer rate. The specific coolant flow (i.e., the coolant mass flow per surface area) calculations indicated a 52 percent reduction of coolant, with respect to a conventional convection film-cooled combustor assumed maximum operating conditions were peak liner temperature of 1200 K (1700 °F) for a stoichiometric primary with hot streaks corresponding to a pattern factor of 0.25 at an average temperature outlet of 1560 K (2348 °F).

Combustor Liner Coolant Comparison

A summary of the percentage of mass flow distribution for outer liner cooling is shown in Fig. 5. The air entry locations are ratioed to the total length of the outer liner from the fuel injector faceplate to the turbine stator location. Flow distributions for the CFFC liner are compared with the referenced SF and TRANS (Lamilloy) liners. The coolant flow for the TRANS liner was estimated by summing the flow from each of the relevant "transpiration" holes and assuming this coolant was admitted at an air entry location corresponding to the CFFC and SF liners.

The total CFFC wall cooling mass flow for the selected design is 30.6 percent. Shown for comparison, the SF liner used 32.5 percent and the TRANS liner used 25.6 percent of the total airflow. The calculated coolant mass flow differed for the three liner wall cooling designs primarily due to the relative efficiency of the cooling scheme, as well as the assumptions used to calculate the heat flux. The two main areas involved which show a rather wide difference in calculated coolant flow are associated with the turn on the outer liner and with the primary zone liner (outer ring). The coolant flow requirements for the CFFC liner in the outer turn is 5.5 percent. This compares to calculated values of 7.05 and 13.92 percent for the TRANS and SF liners, respectively. The calculated flow for the CFFC liner for the outer primary zone panels is 13 percent. This compares to coolant flows of 5.13 and 4.42 percent for the TRANS and SF liners, respectively. It is to be noted that the SF liner primary zone liner temperature levels exceeded the 1200 K (1700 °F) maximum design temperature goal which was specified for both the CFFC and TRANS liner designs.

Instrumentation

The thermocouple placement on the counter-flow film-cooled (CFFC) liner was based on thermal paint indications and liner wall locations representative of primary, secondary, and dilution zones. Thermocouples were also placed in similar locations to those of the splash-film (SF) liner and the transpiration (TRANS) liner. The thermocouple locations are located as shown in Fig. 3. A total of 15 Chromel-Alumel couples were mounted on the cold side of the CFFC liner to monitor liner temperature.

The combustor instrumentation stations are shown in Fig. 6. Five total pressure probes, two static pressure taps, and four Chromel-Alumel thermocouples are located at station 2 to measure the inlet temperature and pressure. At station 3, a series of 18 total pressure probes are installed to determine the inlet-air profile and to determine the extent of any flow disturbance behind the struts which support the centerbody diffuser. At station 4, six pitot-static probes are positioned in the cold-air passages between the combustor liner and combustor housing to determine passage velocity and distribution. At station 5, outlet temperature and pressure measurements are obtained by means of a rotating probe. The probe contains three rakes spaced 120° apart, a five-position radial rake containing PT-PT 13 percent Rd thermocouples, a five-position total pressure rake, and a water cooled gas sampling rake. A 360° travel with sampling at ten degree increments was used for this program.

Procedure

Test Conditions

The experimental reverse flow combustor was operated at test conditions based on a gas-turbine engine cycle with a compressor pressure ratio of 16. A tabulation of the test conditions simulated in this study is given in Table 1.

Data were obtained at combustor inlet conditions simulating sea level take-off (SLTO), cruise, and idle. Simulated flight data were obtained at fuel-air ratios up to approximately 0.026, low power at 0.014, and idle at 0.008. The simulated combustor test conditions are based on a reference velocity of 5.49 m/sec. The reference velocity quoted is based on unidirectional total mass flow and the maximum cross-sectional area of the housing prior to the reverse turn (Fig. 6). Parametric variations in velocity of 5.49, 7.32, and 9.14 m/sec were also obtained during the experimental testing, corresponding to increases of 33 and 66 percent based on the reference of 5.49 m/sec.

The test program was conducted using Jet-A fuel with 18 simplex pressure-atomizing fuel injectors with a flow number of 4.8.

Emission Measurements

Exhaust gas samples were obtained according to the recommended procedures in Refs. 7 and 8. Exhaust gases were withdrawn through the water cooled rotating probe mounted approximately in the stator plane and in the center of the exhaust duct at station 5 (Fig. 6). The gas sample temperature was held at approximately 423 K in the electrically heated sampling line. Most of the gas sample entered the analyzer oven, while the excess fuel was bypassed to the exhaust system. To prevent fuel accumulation in the sample line, a nitrogen purge was used before and during combustor ignition.

After passing through the analyzer oven, the gas sample was divided into three parts, and each part was analyzed. Concentrations of oxides of nitrogen, carbon monoxide and carbon dioxide, and hydrocarbons were measured by the chemiluminescence, nondispersed-infrared, and flame-ionization methods, respectively. Details of the gas analysis system are presented in Ref. 2. The combustion efficiency data presented in this paper were based on stoichiometry determined by gas analysis.

Results and Discussion

A combustor featuring advanced liner cooling techniques and identified as a counter-flow film-cooled (CFFC) combustor was operated at test conditions typical of a 16:1 pressure ratio turbine engine. Combustion efficiency, emissions, outlet temperature distribution, and liner temperature data are compared for simulated flight conditions and a parametric variation of increased combustor loading. Comparison with conventional splash film-cooled (SF) liner walls and a simulated transpiration cooled (TRANS) combustor (Lamilloy) are also included.

Performance

Combustion efficiency. The combustion efficiency data are presented in Fig. 7 for the CFFC combustor. At simulated flight conditions, efficiency levels near 100 percent were obtained. Combustion efficiencies at reduced power are also indicated (i.e., pressure levels of 850 kPa (125 psia) or lower at a constant fuel air ratio of 0.014). At reduced power, the combustion efficiency remained near 100 percent, but started to drop off at pressure levels below 600 kPa (87 psia). The configuration was tested using 18 simplex fuel injectors. As previously reported, the effect of combustion efficiency in the reference SF combustor was dependent on fuel atomization.[2] At low flows, the fuel spray characteristics deteriorate, particularly with simplex pressure atomizing injectors. This deterioration can be countered by either reducing the number of fuel injectors, or using an advanced injector, such as spill flow.[2]

With the SF and TRANS combustors efficiency levels near 100 percent were obtained at simulated flight conditions as shown for reference in Fig. 7. As power level was reduced below 650 kPa (95 psia), combustion became unstable and blowout was subsequently experienced.

While slight differences in combustion efficiency were observed, the combustion characteristics were similar, except that the CFFC configuration was somewhat more stable at reduced fuel flows with the 18 simplex fuel injectors. This may in part be due to the influence of the primary swirler air in providing a somewhat richer primary zone. The design airflow entering into the primary reaction zone was 25.43 percent for the CFFC combustor, as compared to 26.63 percent for the SF configuration, and 26.63 percent for

the TRANS combustor. The measured total pressure for the three different combustor liners were similar (approximately 1.7 percent). Consequently, since air entry placement was geometrically identical, the basic internal aerodynamics and recirculation patterns would be expected to be similar. It was considered that the design transfer from the basic SF to the CFFC configuration was successfully accomplished.

Emissions. Although emission levels are not currently required for the small turbojets, the emission levels are an indication of the effectiveness of the combustion process in relationship to the internal flow and mixing dynamics. Emission index is defined as the grams of pollutant per kilogram of fuel burned. The emission index for the CFFC combustor was less than one for unburned hydrocarbons and less than two for carbon monoxide at simulated flight conditions. At low power, the emission index increased in accordance with the loss in combustion efficiency. The unburned hydrocarbons and carbon monoxide indexes were similar for the SF and TRANS liner configurations.

The oxides of nitrogen (NO_x) emission levels are presented in Fig. 8 for inlet conditions representative of a helicopter cruise condition over a range of fuel-air ratios. As shown, the emission index at a fuel-air ratio of 0.025 for NO_x is 14. For comparison, the emission index of NO_x obtained with the SF and TRANS liners are 18 and 12, respectively. The decrease in NO_x with the CFFC and TRANS combustor liners, as compared to the SF liner, is significant. The results obtained indicate that the NO_x emission is sensitive to the liner cooling technique. For reference at a comparable condition, the NO_x emission index for an advanced low emission turbojet engine combustor is about 14.[9]

The transfer of the basic design to alternative liner cooling techniques involved a number of design compromises in order to maintain equivalent air-entry momentum ratio, hole size, and penetration depth. It was apparent that the internal aerodynamics were not severely compromised due to the fact that the geometric factors were similar, and the combustor performance factors such as efficiency, pressure loss, and stability were also similar.

The major difference between the combustors was in the method of liner cooling. In the sheet metal configuration of the SF reference liner, control is afforded by means of accurately drilled holes to meter the coolant. The resultant protective film is produced by means of a sheet metal annulus; consequently, precise control of the film is not possible.

In the CFFC configuration, the finned heat exchanger is used to transfer excess heat to the coolant, and also provides precise control of the geometric channel height. The resultant film is at a much higher temperature level than the SF film and in addition, the film thickness is accurately controlled. In the TRANS liner, advantage is also taken of the heat sink potential of the coolant which is then used as a film to protect the metallic liner.

The trend in the reduction of NO_x emission level is consistent with improvement in cooling film management. The SF and CFFC liners both rely on continuous film replacement; however, in the CFFC configuration, the coolant has been preheated. In the TRANS configuration, the coolant is also preheated, and in addition the film more effectively distributed. Indications are that preheating of the coolant film affects the internal aerodynamics so as to provide more efficient mixing of the fuel and air. Uniform mixing can be beneficial in reducing NO_x emission for a given design stoichiometry.

Rationale with respect to reduced NO_x emission with the TRANS configuration was believed to be due to improvements in fuel-air uniformity as a result of better mixing.[5] The factors which contributed to improved mixing in the TRANS configuration were due to minimum interaction of the primary air admission sources with the film coolant. In the present study, a greater interaction with the air admission sources and the film would be expected (i.e., 13 percent primary zone wall coolant as compared to 5.2 percent). However, in the CFFC case, the film air is preheated to temperatures approaching the liner wall temperature (see Fig. 13). In the more conventional SF design, the film inlet can be approximated at the compressor discharge level. Mixing of the coolant film and the hot combustion gases does occur. Indications are in the CFFC configuration that this mixing need not be detrimental, and that the hotter film temperature improved the internal mixing characteristics to provide more uniform combustion.

Outlet temperature distribution. The outlet temperature distribution as indicated by pattern factor is shown over a range of fuel-air ratios for simulated sea level take off (SLTO) in Fig. 9. Pattern factor (PF) is defined as:

$$PF = \frac{T_{max} - T_{ave}}{T_{ave} - T_{inlet}}$$

Where T_{max} is the highest temperature recorded from the exhaust tranversing rake; T_{ave}, the average exhaust temperature; and T_{inlet}, the combustor inlet temperature. At simulated rated power for the SLTO condition, the pattern factor was 0.27 for the CFFC combustor. This compares with 0.31 and 0.17 for the SF and TRANS liner combustors, respectively. While the effect of coolant film preheat improved PF at reduced fuel flow, there appeared to be minimal improvement with respect to the outlet temperature distribution at full power.

A color graphic simulation of the combustor exhaust is shown for the SLTO condition in Fig. 10. Temperatures range from 1316 K (1907 °F) as a minimum to a peak level of 1755 K (2699 °F) for an average outlet of 1549 K (2328 °F). No attempt was made in any of the liner cooling studies to control pattern factor.

Parametric variation of reference velocity. The effect of increasing the mass flow for a given inlet pressure and temperature in the reverse flow combustor was investigated to determine the effect on performance factors. Nominal mass flow increases of 33 and 67 percent were tested at simulated basic turbojet engine conditions. An increase in mass flow at constant inlet pressure and temperature is directly related to reference velocity.

The combustion efficiency with the CFFC liner was not appreciably affected by an increase in reference velocity. As with the SF and TRANS liners, the combustion efficiency obtained with the CFFC liner remained substantially at 100 percent.

Emission levels of NO_x a shown in Fig. 11. A more marked decrease was experienced with the CFFC liner as compared to the SF liner at the SLTO condition than noted at simulated cruise (Fig. 8). As the reference velocity was increased, a slight increase in NO_x was indicated; however, at a 67 percent increase in reference velocity, both the CFFC and TRANS configurations produced about the same level of NO_x (10.7 g/kg). The decrease in NO_x ith the CFFC liner is attributed to improved nternal mixing as a result of interaction of the "hotter" film and the combustible mixture, as well as, the fact that at higher velocities the pressure drop across the liner increases, resulting in additional mixing potential.

Outlet temperature distribution as indicated by pattern factor was relatively unaffected by an increase in reference velocity as shown in Fig. 12. By comparison, both the SF and TRANS liners experienced an increase in pattern factor with increased reference velocity.

Liner Temperature

Liner wall temperature prediction. The combustor liner wall temperature calculation was performed using a one-dimensional computational scheme. The analysis included convection and radiation heat transfer contributions from the hot gas and the annulus sides, film cooling efficiency along the wall, and the change of area, wall thickness, and materials.

For computational purposes, the liner wall was divided into independent sections. For each section, a fuel-air ratio was computed from the total amount of air and fuel present at the section. Only the effect of the cooling film was excluded for the panel being evaluated, since the cooling film serves to cool the liner and does not interact with the burning process; however, the cooling film flow rate was taken into account on the next downstream panel, where the flow was assumed to be mixed completely with the hot gases.

The flame temperature (T_{ft}) was estimated from the adiabatic flame temperature corresponding to the known fuel-air ratio and a combustion efficiency of 90 percent in the primary zone and 100 percent in the remainder of the combustion chamber.

Based upon the results from the annular flow distribution, the CFFC combustor displayed a typical profile calculated from the Garrett program as shown in Fig. 13 for the outer and inner cylindrical sections.[4] The design indicates that the maximum liner design temperatures of 1200 K (1700 °F) would not be exceeded.

Shown in Fig. 14 is a thermal paint photograph of the liner after "firing" at the simulated SLTO condition. The average temperature indication was about 1030 K (1400 °F). The highest temperature levels were noted downstream of the fuel injectors on the outer second dilution panel. In general, a very uniform temperature indication was noted for all panels, and the temperature level observed from the thermal paint indications compares favorably with the temperature predictions as shown in Fig. 13.

Liner cooling effectiveness. The effect of combustor operating conditions and increased loading on liner cooling effectiveness is shown in Fig. 15. For comparative purposes, the cooling effectiveness (n_c) is defined as:

$$n_c = \frac{T_{flame} - T_{wall}}{T_{flame} - T_{coolant}}$$

Where n_c is the film cooling effectiveness, T_{flame} is the flame temperature, T_{wall} is the wall temperature, and $T_{coolant}$ is assumed to be the coolant inlet air temperature. The results shown in Figs. 15(a) and (b) are typical of those obtained from thermocouple locations on the second dilution panel both inline and between fuel injectors and on the outer and inner turns. Values of film cooling effectiveness over the range from 0.74 to 0.99 were obtained as the inlet pressure was increased from 1000 to 1600 kPa. The coolant inlet temperature was based on that obtained from an adiabatic compression 80 percent efficient and operation at a fuel-air ratio of 0.026.

Cooling effectiveness values increased somewhat as the combustor pressure increased as shown in Fig. 15(a). This would be expected since conditions are more favorable for convective heat transfer and the radiative load would not be expected to increase unless soot formation became excessive.

The effect of a parametric increase in combustor velocity at a constant pressure and temperature corresponding to SLTO inlet conditions is shown in Fig. 15(b). The combustor velocity corresponds to an increase of 33 and 66 percent in mass flow as compared to the reference condition. In general, a slight improvement in film cooling effectiveness is indicated as the combustor reference velocity is increased. The experimental values indicate that the combustor liner can tolerate increased loading. However, it should be noted that increased loading is accompanied by an increase in pressure drop across the liner. For this case, the isothermal loss increased from 1.7 to 3.7 percent.

Comparison of the cooling film effectiveness with that predicted from the Garrett computer program is shown in Fig. 16 at five stations along the liner ranging from 28 to 80 percent of the liner length. There was no general consistency of the data with that predicted. In some regions, film cooling efficiency was higher than expected, and in other regions less. However, the general range was favorable indicating that the design correlations for the CFFC combustor liner were applicable.

The experimental cooling effectiveness for the CFFC liner is compared with the SF and TRANS configurations in Fig. 17 for the outer turn section. As shown, the CFFC and TRANS configurations were similar. As with the TRANS liner, the CFFC liner used approximately 50 percent less air than the SF liner for this series of panels. As shown in Ref. 10, the CFFC technique has the potential to be as effective as a transpiration film. The results from this study indicate that the potential for cooling air reduction as predicted by an

analysis of liner cooling schemes can be realized with experimental hardware.

Conclusions

1. The transfer and use of the basic NASA reverse-flow combustor design to accommodate different liner cooling schemes was successfully accomplished using existing design procedures.

2. Combustor performance parameters appear to be affected by the technique used for liner cooling. Transpiration cooling offered the most improvement in outlet temperature and emissions; however, preheating of the coolant as in the counter-flow film-cooled design also improved performance as compared to the baseline splash film design. Combustion efficiency and pressure loss were unaffected.

3. The experimental liner cooling effectiveness was similar to that predicted for the configuration by the Garrett computer code.

4. The cooling effectiveness predicted from an analysis of advanced cooling schemes was achieved in combustor liner hardware. Both the CFFC and TRANS techniques were equally effective. Comparison was based on the outer turn which has the largest integral surface area in a reverse flow combustor. Both the CFFC and TRANS liners were designed with 50 percent less coolant than the SF liners in this region.

References

1. Demetri, E.P., Topping, R.F., and Wilson, R.P., Jr., "Study of Research and Development Requirements of Small Gas-Turbine Combustors," Arthur D. Little, Inc., Cambridge, MA, ADL-83381-2, Jan. 1980, (NASA CR-159796).

2. Norgren, C.T., and Riddlebaugh, S.M., "Effect of Fuel Injector Type on Performance and Emission of Reverse-Flow Combustor," NASA TP-1945, 1981.

3. "Computer Program for the Analysis of Annular Combustors," Volume 1, Northern Research and Engineering Corp., Cambridge, MA, Report 1111-1, Jan. 1968, (NASA CR-167922).

4. "Design Documentation Report Counterflow Film-cooled Combustor Program," Garrett Turbine Engine Co., Phoenix, AZ, Report 21-4007-A, June 1982, (NASA CR-167922).

5. Norgren, C.T., and Riddlebaugh, S.M., "Small Gas Turbine Combustor Study - Combustor Liner Evaluation," AIAA Paper 83-0337, Jan. 1983.

6. Dirling, R.B., Jr., "A Method for Computing Roughwall Heat-Transfer Rates on Reentry Nosetips," AIAA Paper 73-763, July 1973.

7. "Control of Air Pollution from Aircraft Engines Emission Standards and Test Procedures for Aircraft," Federal Register, Volume 38, No. 136, Pt. 2, Tuesday, July 17, 1973, pp 19088-19103.

8. "Procedure for the Continuous Sampling and Measurement of Gaseous Emissions from Aircraft Turbine Engines," SAE ARP-1256, Oct. 1971.

9. Jones, R.E., "Selected Results from Combination Research at the NASA Lewis Research Center," NASA TM-82627.

10. Colladay, R.S., "Analysis and Comparison of Wall Cooling Schemes for Advanced Gas Turbine Applications," NASA TN D-6633, 1972.

TABLE 1. - REVERSE-FLOW-COMBUSTOR TEST CONDITIONS

Test condition	Total airflow		Inlet pressure		Inlet temperature		Reference[a] velocity		Simulated compressor pressure ratio	Comments
	kg/sec	lb/sec	kPa	psia	K	°F	m/sec	ft/sec		
A	2.27	5	1014	147	686	775	5.5	18	10	High-altitude cruise
B	3.05	6.71	1358	197	703	805	5.5	18	13.4	Low-altitude cruise
C	3.63	8	1620	235	717	830	5.5	18	16	Sea level take-off (SLTO)
D	1.23	2.70	405	58.5	474	394	5.2	16.9	4	Idle: f/a = 0.008
E	2.12	4.66	862	125	627	668	5.5	18	8.5	Simulated reduced power
F	1.83	4.02	689	100	581	585	---	---	6.8	
G	1.51	3.33	517	75	526	486	---	---	5.1	
H	1.23	2.70	414	60	474	394	---	---	4.1	

[a]Parametric variation based on increase in mass flow to provide increases of 33 and 66 percent in reference velocity.

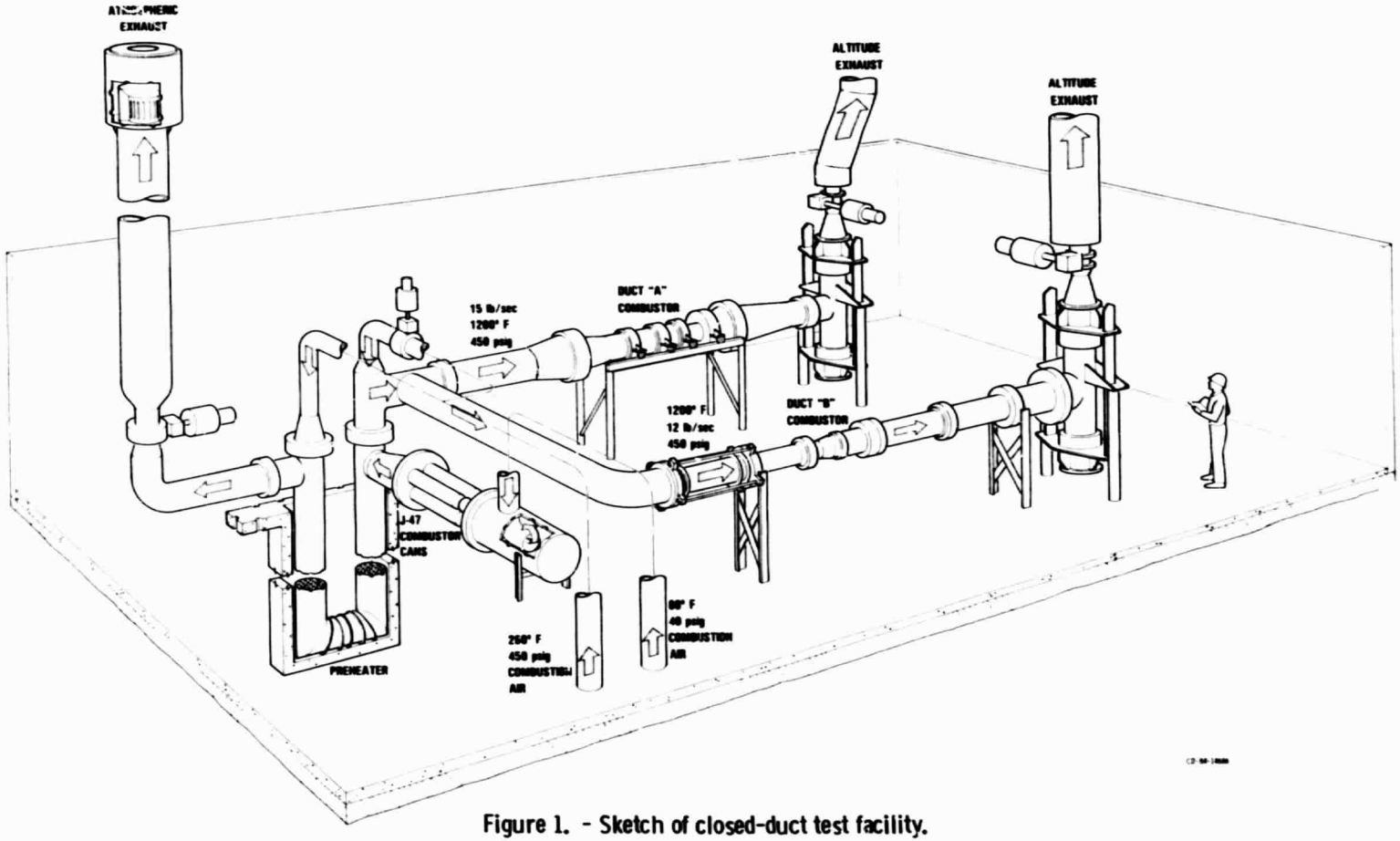

Figure 1. - Sketch of closed-duct test facility.

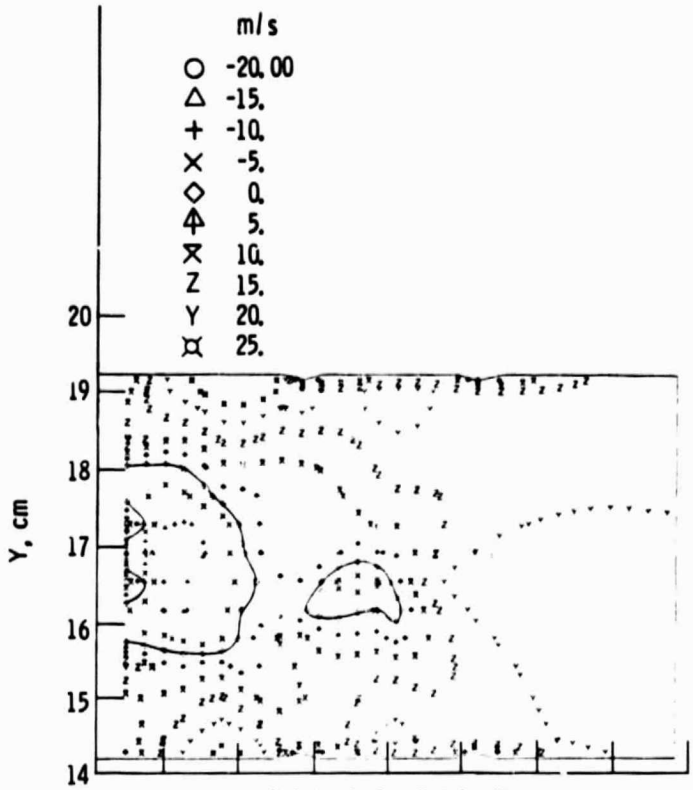

(a) Axial velocity distribution.

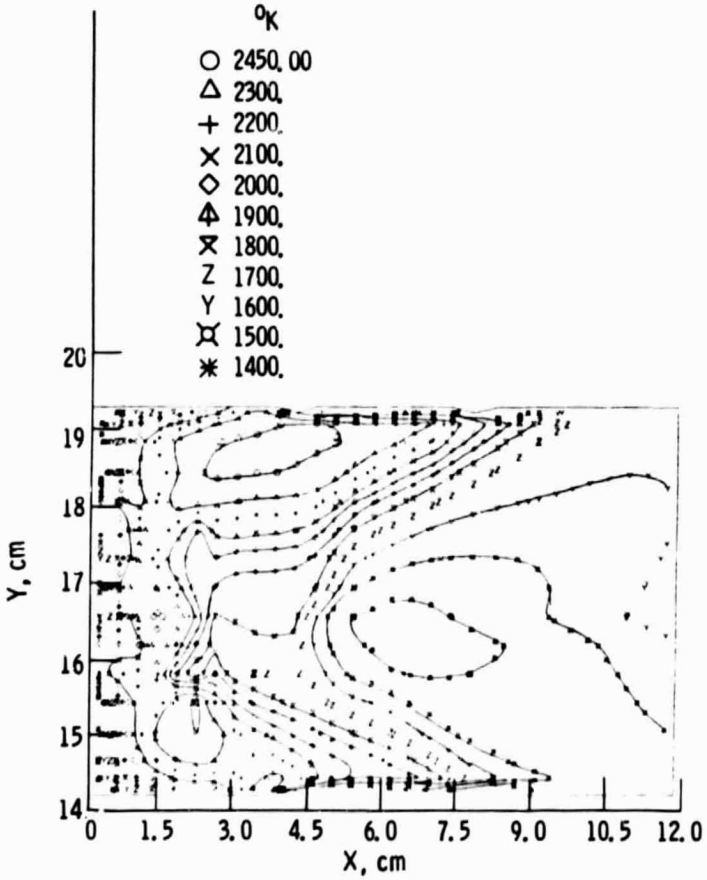

(b) Temperature distribution.

Figure 2. - Examples of the Garrett computer code printout (4) for a plane in-line with the fuel spray.

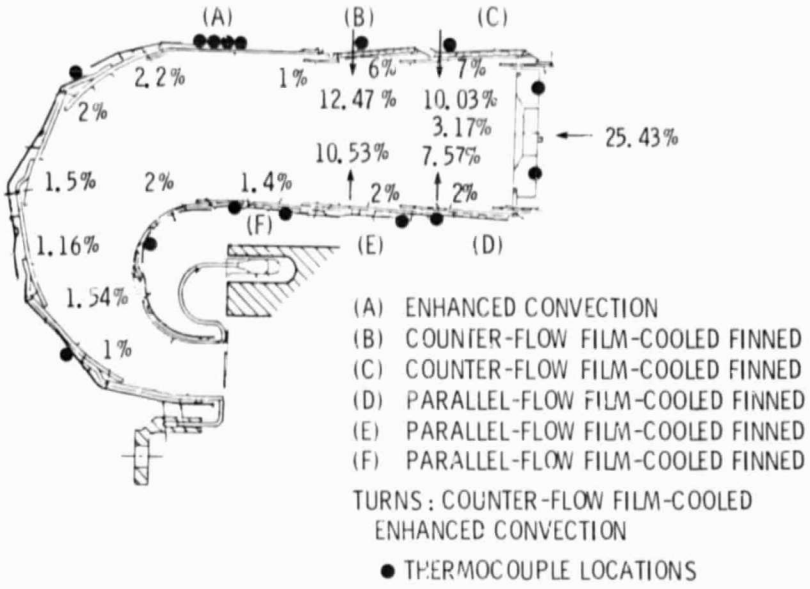

Figure 3. - Cross-sectional view of counter-flow film-cooled reverse flow combustion liner including calculated air-flow distribution.

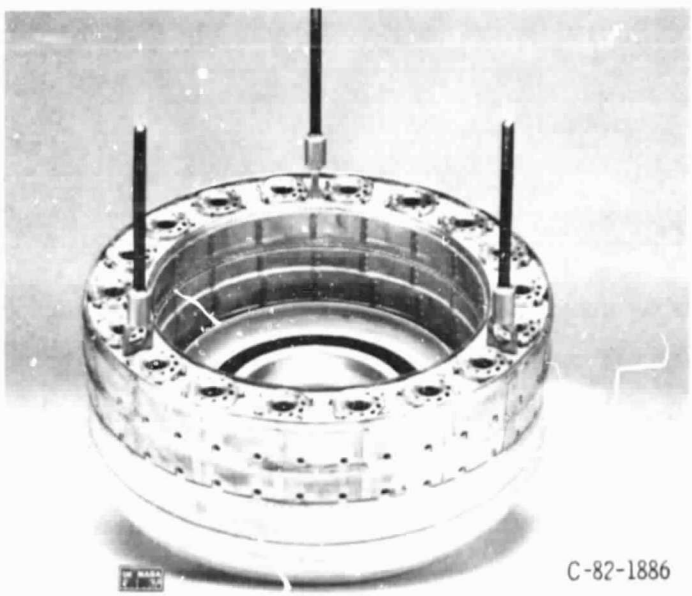

Figure 4. - Completed Counter-flow film-cooled combustor.

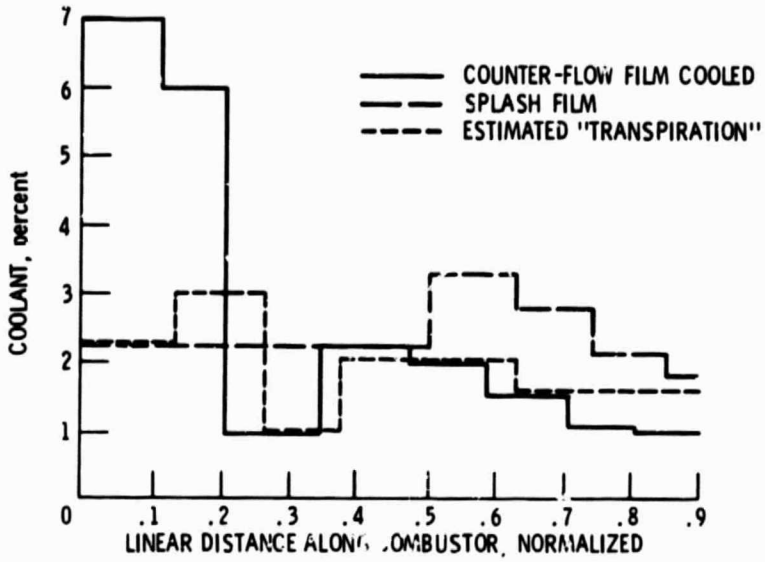

Figure 5. - Coolant mass flow distribution, outer combustor liner wall.

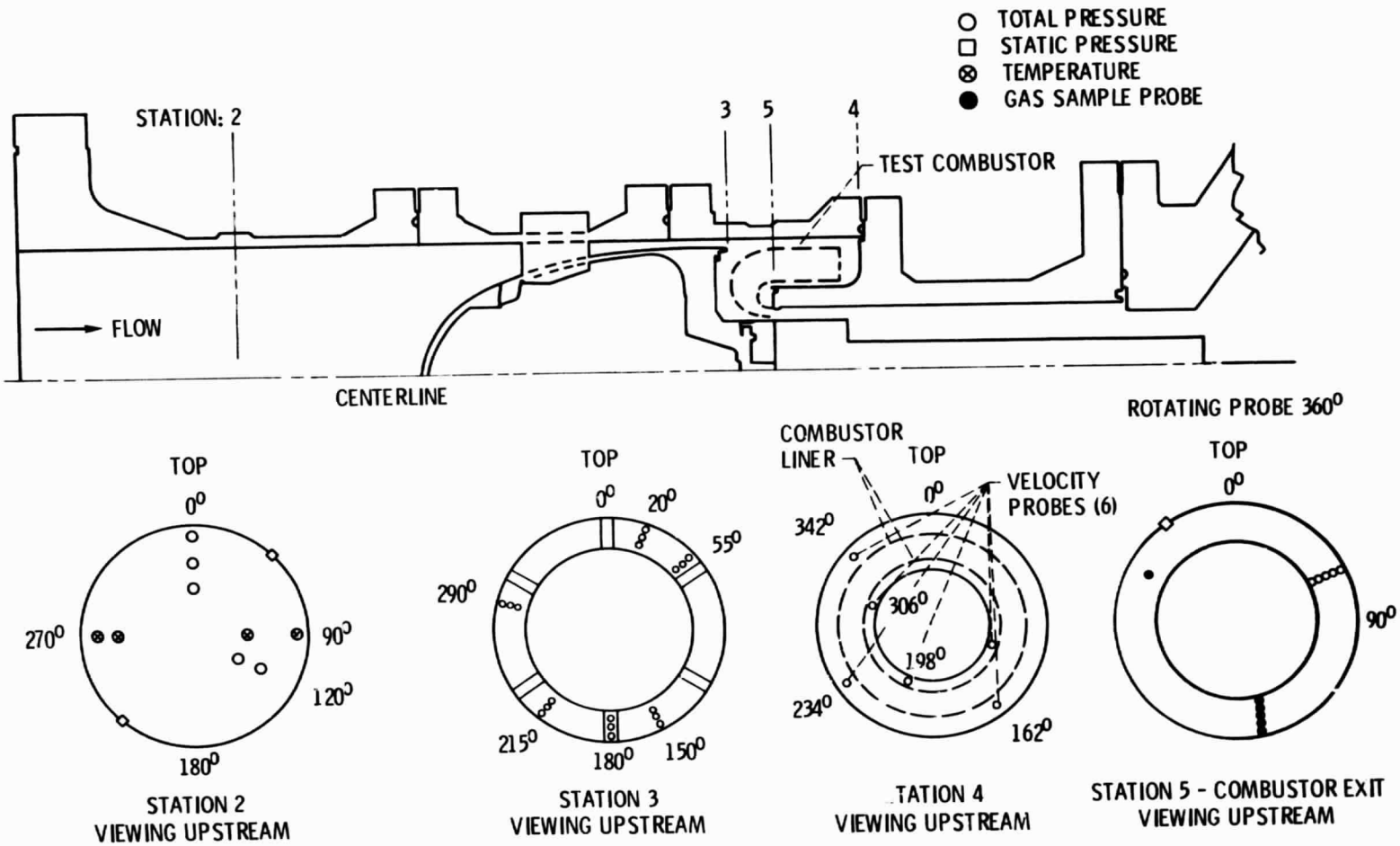

Figure 6. - Research instrumentation.

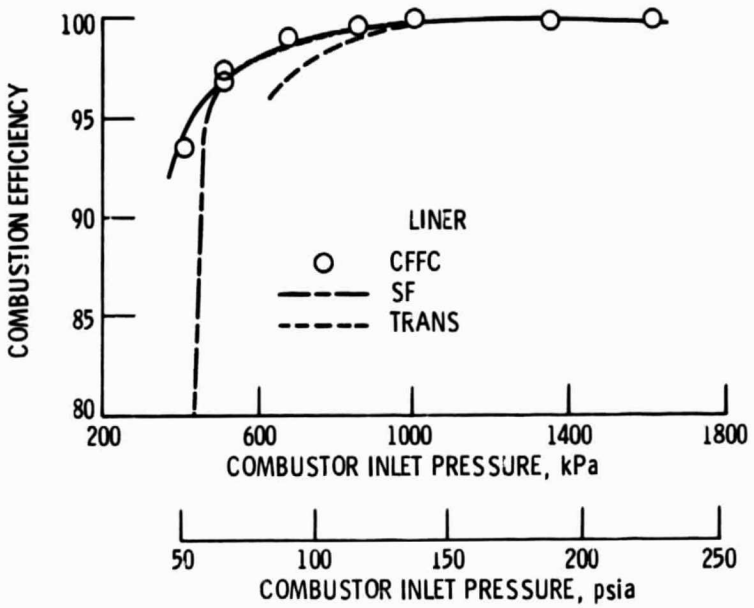

Figure 7. - Counter-flow film-cooled combustor efficiency and comparison with splash film and 'transpiration' liner configurations.

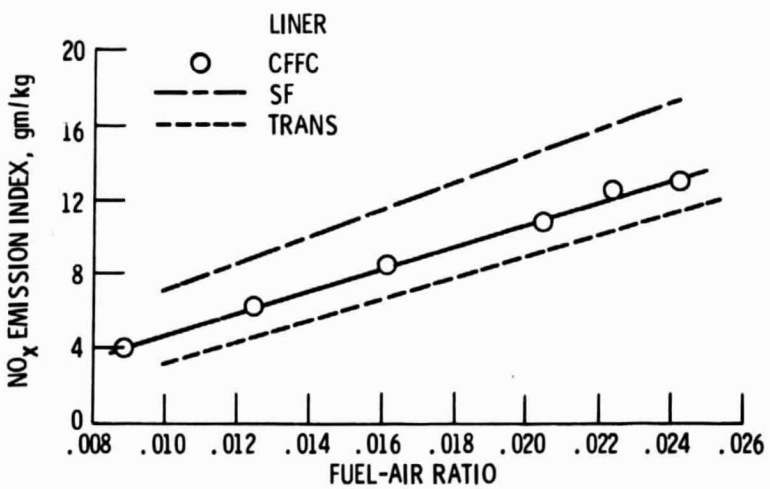

Figure 8. - Comparison of oxides of nitrogen emission from a counter-flow film-cooled (CFFC) liner with a splash film (SF) liner and a Lamilloy (TRANS) liner. (Simulated cruise 16:1 pressure ratio turbojet).

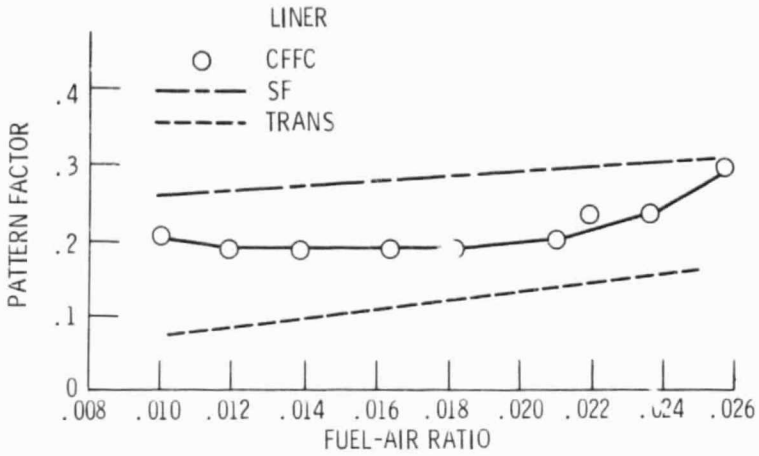

Figure 9. - Comparison of pattern factor from a counter-flow film-cooled (CFFC) liner with a splash film (SF) liner and a Lamilloy (TRANS) liner. (Simulated SLTO 16:1 pressure ratio turbojet.)

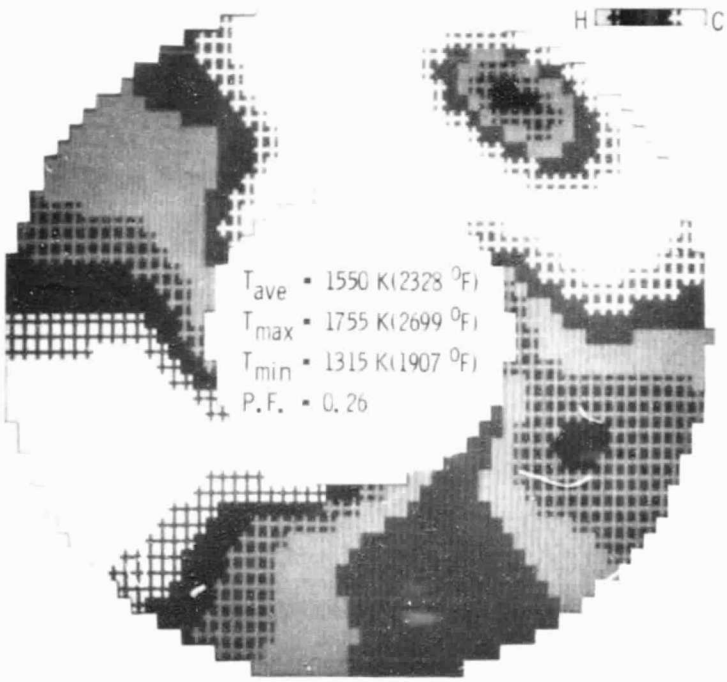

Figure 10. - Outlet temperature distribution at simulated S. L. T. O. for the counter-flow film-cooled combustor.

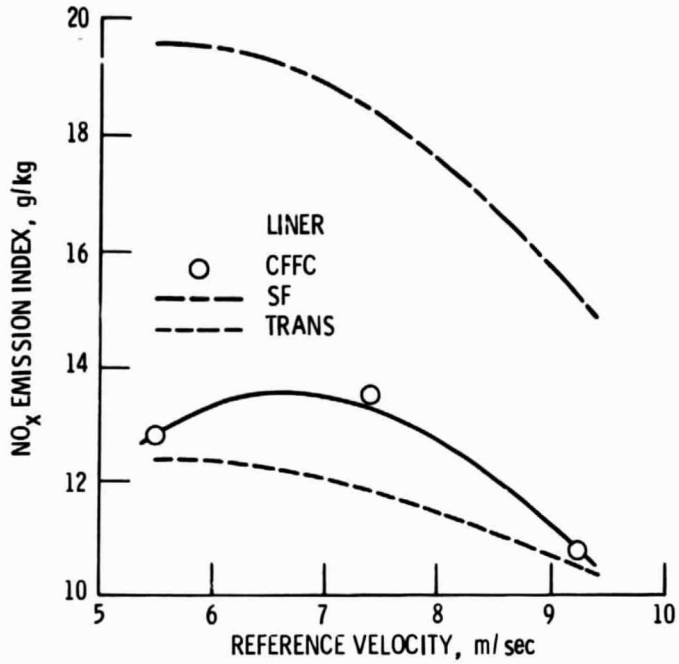

Figure 11. - Effect of parametric variation of reference velocity on NOx emission for a counter-flow film-cooled (CFFC) liner and comparison with a splash film (SF) liner and a Lamilloy (TRANS) liner. (Simulated SLTO 16:1 pressure ratio turbojet engine, f/a = .024).

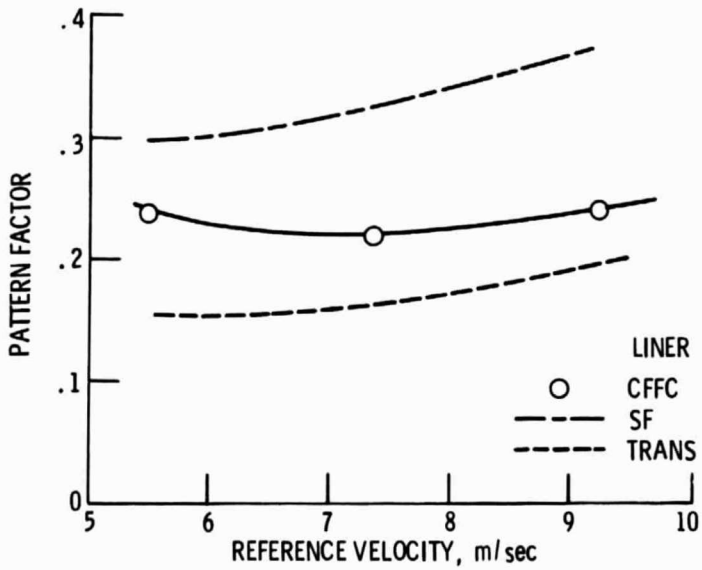

Figure 12. - Effect of parametric variation of reference velocity on pattern factor for a counter-flow film-cooled (CFFC) liner and comparison with a splash film (SF) liner and a Lamilloy (TRANS) liner. (Simulated SLTO 16:1 pressure ratio turbojet engine, f/a = .024).

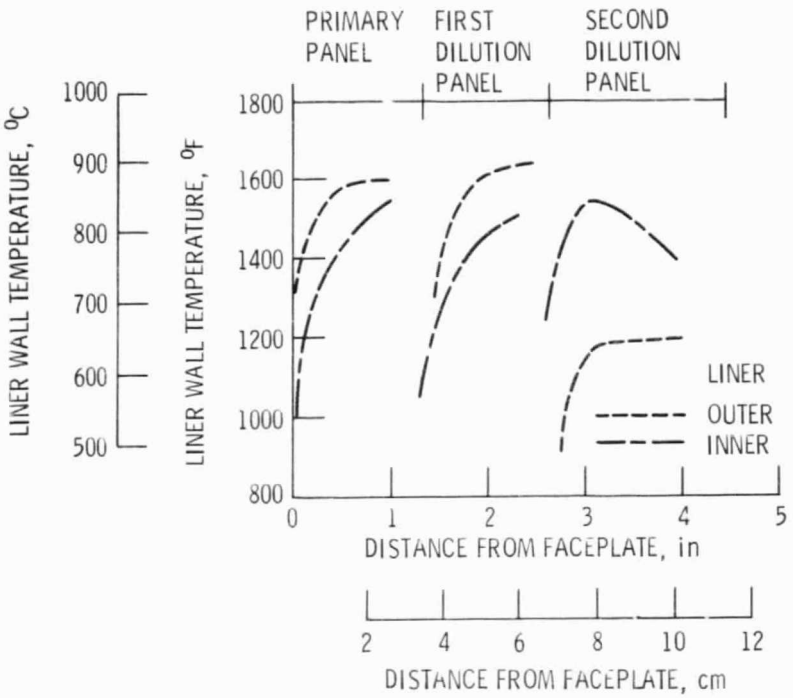

Figure 13. - Calculated temperature distribution counter-flow film-cooled liner. (4).

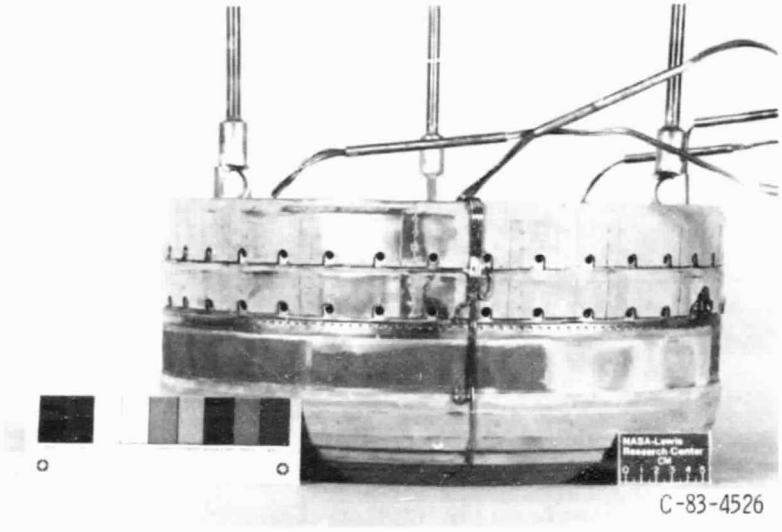

Figure 14. - Indication of liner wall temperature with thermal paint.

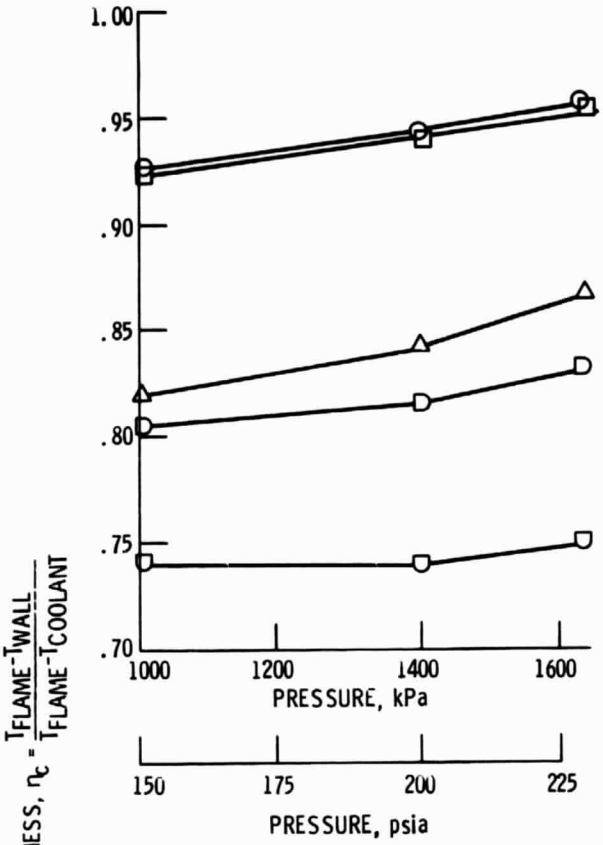

(a) Effect of increased power.

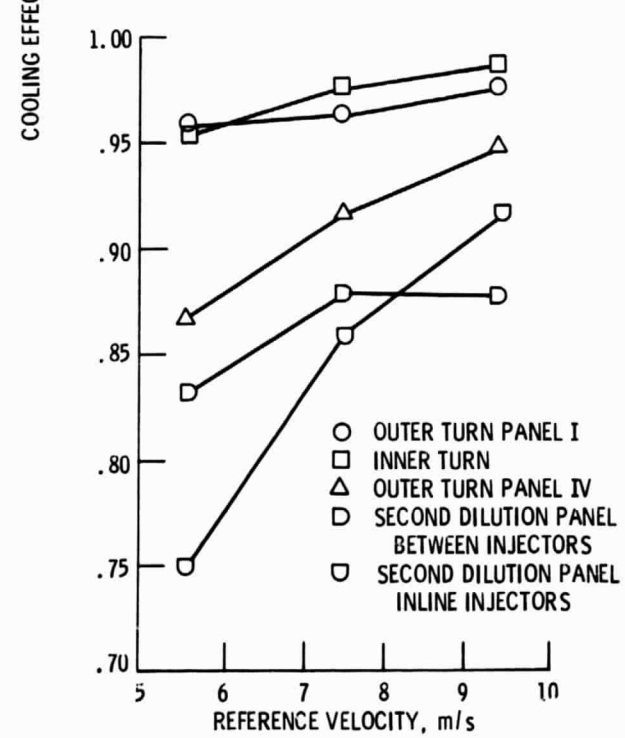

(b) Effect of increased loading on SLTO condition.

Figure 15. - Effect of inlet pressure and velocity on cooling effectiveness.

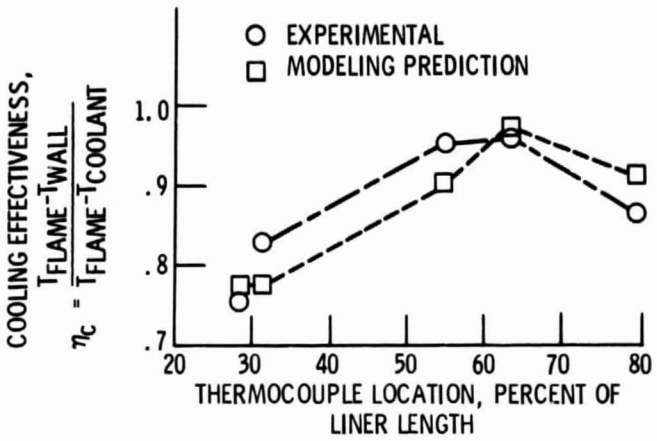

Figure 16. - Comparison of experimentally determined cooling effectiveness with modeling prediction. (Simulated SLTO 16:1 pressure ratio turbojet.)

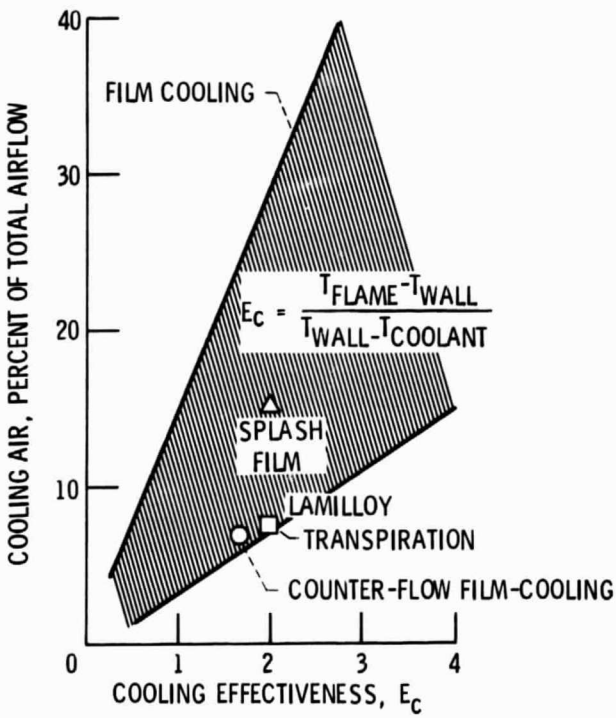

Figure 17. - Comparison of cooling effectiveness from a counter-flow film-cooled liner with a splash film and a Lamilloy liner for the outer turn section.